Structure of Inhomogeneous Attractive and Repulsive Hard-Core Yukawa Fluid: Grand Canonical Monte Carlo Simulation and Density Functional Theory Study

Feng-Qi You, Yang-Xin Yu,* and Guang-Hua Gao

Department of Chemical Engineering, Tsinghua University, Beijing 100084, People's Republic of China, and State Key Laboratory of Chemical Engineering, Tsinghua University, Beijing 100084, People's Republic of China

Received: October 26, 2004; In Final Form: December 10, 2004

A density functional theory is proposed for an inhomogeneous hard-core Yukawa (HCY) fluid based on Rosenfeld's perturbative method. The excess Helmholtz energy functional is derived from a modified fundamental measure theory for the hard-core repulsion and a quadratic functional Taylor expansion for the long-ranged attractive or repulsive interactions. To test the established theory, grand canonical ensemble Monte Carlo simulations are carried out to simulate the density profiles of attractive and repulsive HCY fluid near a wall. Comparison with the results from the Monte Carlo simulations shows that the present density functional theory gives accurate density profiles for both attractive and repulsive HCY fluid near a wall. Both the present theory and simulations suggest that there is depletion for attractive HCY fluid at low temperature, but no depletion is found for repulsive HCY fluid. The calculated results indicate that the present density functional theory is better than those of the modified version of the Lovett−Mou−Buff−Wertheim and other density functional theories. The present theory is simple in form and computationally efficient. It predicts accurate radial distribution functions of both attractive and repulsive HCY fluid except for the repulsive case at high density, where the theory overestimates the radial distribution function in the vicinity of contact.

I. Introduction

The structure of fluids at interfaces is very important in many applications such as absorption, wetting, capillary condensation, etc. Many theoretical methods have been proposed for inhomogeneous hard-sphere fluid[1−5] and Lennard-Jones fluid.[6,7] However, in this work we consider the fluid with attractive or repulsive Yukawa potential due to its wide applications to simple fluids, charge-stabilized colloidal suspensions,[8,9] micelles,[10,11] microemulsions,[12] dense plasmas,[13] and C_{60} molecular systems.[14] The hard-core Yukawa (HCY) potential is given by

$$u(r) = \begin{cases} \infty & , r < \sigma \\ -\dfrac{\epsilon \exp[-\lambda(r/\sigma - 1)]}{r/\sigma} & , r \geq \sigma \end{cases} \qquad (1)$$

where σ is the diameter of particles, ϵ is the potential energy at contact, λ is a screening length for the Yukawa tail, and r is the center-to-center distance between two interacting particles. When $\epsilon > 0$, eq 1 represents attractive HCY fluid, while it is for repulsive HCY fluid when $\epsilon < 0$.

Many studies have been carried out to investigate the phase equilibria, thermodynamic properties, and surface tension of the attractive hard-core Yukawa (HCY) fluid,[12,15−17] while few works were done for the repulsive HCY fluid. Recently, Cochran and Chiew[18] investigated the thermodynamic and structural properties of repulsive hard-core Yukawa fluid using integral equation theory, perturbation theory, and Monte Carlo simulations. As for the inhomogeneous HCY fluid, Olivaves-Rivas et al.[19] used the singlet hypernetted chain (HNC) integral equation and a modified version of the Lovett−Mou−Buff−Wertheim (LMBW-1) to predict the density profile near a hard wall at reduced density $\rho\sigma^3 = 0.7$. The comparison with their own data showed that the LMBW-1 equation works well at high temperatures and overestimates density profiles at low temperatures. Soon after, Yi and Kim[20] proposed a density functional perturbative approximation for attractive HCY fluid, which is based on the weighted-density approximation (WDA) of Tarazona[21,22] and the density functional approximation of Rickayzen et al.[23,24] Because the correct total pressure of the homogeneous fluid is used in the determination of the value of the strength parameter of their theory, it gives correct contact value, but weaker oscillations when compared with the simulation data. Another perturbation density functional theory[25] also uses the bulk pressure for uniform Yukawa fluid to determine its parameter. So far, all the studies for inhomogeneous attractive HCY fluid are limited to the reduced density $\rho\sigma^3 = 0.7$, and no investigation on confined repulsive HCY fluid was reported.

Density functional theory (DFT) is a powerful tool to study the structure properties of inhomogeneous fluids. The key problem of a DFT is that there is no exact form of the Helmholtz free-energy functional. Besides Tarazana's WDA,[21,22] the fundamental measure theory of Rosenfeld,[2] especially the latest modified version (MFMT),[3,4] yields very accurate density profiles for the fluids with solely repulsive forces near walls and inside slit pores as well as the radial distribution functions for homogeneous hard spheres and mixtures. The most simple and popular method for dispersion force is the so-called mean-field theory (MFT),[1] which is computationally efficient but describes some inhomogeneous phenomena only qualitatively. The usual way to correct the results from MFT is the bulk fluid direct correlation function obtained from the integral equation theory. In this work, we reformulate the Helmholtz free-energy function for the inhomogeneous attractive and repulsive HCY

* To whom correspondence should be addressed. E-mail: yangxyu@mail.tsinghua.edu.cn.

10.1021/jp045112h CCC: $30.25
Published on Web 02/05/2005

fluid through Rosenfeld's perturbative method.[26] The excess Helmholtz free-energy function due to hard-sphere repulsion is evaluated from the MFMT, and dispersion contribution is obtained using a quadratic expansion of the Helmholtz free-energy function with respect to that for a uniform fluid of the same chemical potentials. Then the theory is applied to investigating the density profiles of attractive and repulsive HCY fluid near a wall and the radial distribution functions of homogeneous HCY fluid. To test the prediction of the present DFT, the grand canonical ensemble Monte Carlo (GCMC) simulations have been carried out to obtain the density profiles of attractive and repulsive HCY fluid near a wall at different reduced temperatures and densities.

In what follows, we present the DFT theory for HCY fluid in Section II, the Monte Carlo method in Section III, the numerical results for the density profiles and the radial distribution functions in Section IV, and a few general conclusions in Section V.

II. Density Functional Theory

The grand potential for an inhomogeneous Yukawa fluid is related to the Helmholtz energy functional through the Legendre transform

$$\Omega[\rho(\mathbf{r})] = F[\rho(\mathbf{r})] + \int d\mathbf{r}[V_{ext}(\mathbf{r}) - \mu]\rho(\mathbf{r}) \tag{2}$$

where $\rho(\mathbf{r})$ is density profile for a Yukawa fluid, μ is the chemical potential, Ω is the grand potential, $V_{ext}(\mathbf{r})$ is the external potential, and F is the intrinsic Helmholtz energy functional. Without loss of generality, we decompose F into ideal and excess parts

$$F[\rho(\mathbf{r})] = F^{id}[\rho(\mathbf{r})] + F^{ex}[\rho(\mathbf{r})] \tag{3}$$

where the ideal intrinsic Helmholtz energy is known exactly,

$$F^{id}[\rho(\mathbf{r})] = k_B T \int d\mathbf{r}[\ln(\rho(\mathbf{r})\lambda^3) - 1]\rho(\mathbf{r}) \tag{4}$$

In eq 4, k_B is the Boltzmann constant, T is the absolute temperature, and λ is the thermal de Broglie wavelength of the HCY spheres.

The central topic of a density functional theory is to derive an analytical expression for the excess Helmholtz free energy as a functional of the density distributions. The excess Helmholtz free energy can be further decomposed into the contributions from the hard-sphere repulsion and long-ranged attraction.

$$F^{ex}[\rho(\mathbf{r})] = F^{ex}_{hs}[\rho(\mathbf{r})] + F^{ex}_{att}[\rho(\mathbf{r})] \tag{5}$$

As in the previous work, we apply the MFMT[3,4] for the functional $F^{ex}_{hs}[\rho(\mathbf{r})]$ in eq 5. The mathematical expression of the MFMT excess Helmholtz free-energy functional is given by

$$\beta F^{ex}_{hs} = \int \Phi^{hs}[n_\alpha(\mathbf{r})]d\mathbf{r} \tag{6}$$

where $\Phi^{hs}[n_\alpha(\mathbf{r})]$ is the reduced excess Helmholtz free-energy density due to hard-sphere repulsion, $\beta = 1/k_BT$, and $n_\alpha(\mathbf{r})$ is the weighted density. The definition of the weighted densities can be found in the previous work and papers of Rosonfeld.[2] In MFMT, the hard-sphere Helmholtz free-energy density consists of contributions from the scalar-weighted densities and the vector-weighted densities,

$$\Phi^{hs}[n_\alpha(\mathbf{r})] = \Phi^{hs(S)}[n_\alpha(\mathbf{r})] + \Phi^{hs(\mathbf{V})}[n_\alpha(\mathbf{r})] \tag{7}$$

where the superscripts (S) and ($\mathbf{V}$) stand for the contributions from scalar- and vector-weighted densities, respectively. The scalar Helmholtz energy density is given by

$$\Phi^{hs(S)}[n_\alpha(\mathbf{r})] = -n_0\ln(1-n_3) + \frac{n_1 n_2}{1-n_3} + \frac{n_2^3\ln(1-n_3)}{36\pi n_3^2} + \frac{n_2^3}{36\pi n_3(1-n_3)^2} \tag{8}$$

and the vector part is expressed by[3,4]

$$\Phi^{hs(\mathbf{V})}[n_\alpha(\mathbf{r})] = -\frac{\mathbf{n}_{V1}\mathbf{n}_{V2}}{1-n_3} - \frac{n_2\mathbf{n}_{V2}\mathbf{n}_{V2}\ln(1-n_3)}{12\pi n_3^2} - \frac{n_2\mathbf{n}_{V2}\mathbf{n}_{V2}}{12\pi n_3(1-n_3)^2} \tag{9}$$

In the limit of a bulk fluid, the two vector-weighted densities $\mathbf{n}_{V1}$ and $\mathbf{n}_{V2}$vanish, and the Helmholtz free-energy density Φ^{hs} becomes identical to that from the Boublik−Mansoori−Carnahan−Starling−Leland (BMCSL)[27,28] equation of state.

To obtain the contribution of long-ranged attractive or repulsive force to the excess Helmholtz energy functional, Rosenfeld[26] assumed that it could be perturbatively constructed around that for the bulk fluid at equilibrium. Therefore, we can make a functional Taylor expansion of the residual Helmholtz free-energy functional around that for a uniform fluid to obtain

$$F^{ex}_{att}[\rho(\mathbf{r})] = F^{ex}_{att}(\rho_b) + \int \frac{\delta F^{ex}_{att}}{\delta\rho(\mathbf{r})}[\rho(\mathbf{r}) - \rho_b]d\mathbf{r} + \frac{1}{2}\int\int d\mathbf{r}\, d\mathbf{r}' \frac{\delta^2 F^{ex}_{att}}{\delta\rho(\mathbf{r})\delta\rho(\mathbf{r}')}[\rho(\mathbf{r}) - \rho_b][\rho(\mathbf{r}') - \rho_b] + ... \tag{10}$$

where ρ_b is the bulk density. The direct correlation functions due to the residual attraction are defined as

$$\Delta C^{(1)}_{att} = -\beta\frac{\delta F^{ex}_{att}}{\delta\rho(\mathbf{r})} \tag{11}$$

$$\Delta C^{(2)}_{att}(|\mathbf{r}' - \mathbf{r}|) = -\beta\frac{\delta^2 F^{ex}_{att}}{\delta\rho(\mathbf{r})\,\delta\rho(\mathbf{r}')} \tag{12}$$

If we neglect all higher-order term $\Delta C^{(n)}_{att}$ ($n > 2$) in eq 10, $F^{ex}_{att}[\rho(\mathbf{r})]$ becomes

$$\beta F^{ex}_{att}[\rho(\mathbf{r})] = \beta F^{ex}_{att}[\rho_b] - \int \Delta C^{(1)}_{att}[\rho(\mathbf{r}) - \rho_b]d\mathbf{r} - \frac{1}{2}\int\int d\mathbf{r}\, d\mathbf{r}'\Delta C^{(2)}_{att}(|\mathbf{r}' - \mathbf{r}|)[\rho(\mathbf{r}) - \rho_b][\rho(\mathbf{r}') - \rho_b] + ... \tag{13}$$

At the equilibrium, the grand potential $\Omega[\rho(\mathbf{r})]$ reaches its minimum, i.e., $\delta\Omega[\rho(\mathbf{r})]/\delta\rho(\mathbf{r}') = 0$. The following Euler−Lagrange equation for the density profile can be achieved.

$$-\ln\left[\frac{\rho(\mathbf{r})}{\rho_b}\right] = \beta\left[\frac{\delta F^{ex}_{hs}}{\delta\rho(\mathbf{r})} - \mu^{ex}_{hs}\right] + \beta V_{ext}(\mathbf{r}) - \int d\mathbf{r}'\Delta C^{(2)}_{att}(|\mathbf{r}' - \mathbf{r}|)[\rho(\mathbf{r}') - \rho_b] \tag{14}$$

where F^{ex}_{hs} is evaluated from eq 6, and μ^{ex}_{hs} is the chemical potential due to hard-sphere repulsion, which can be obtained from the Carnahan−Starling equation. The perturbative method is completely free of any weighted density and of any higher-

order DCFs, as appeared in many other DFTs. The excess direct correlation function $\Delta C^{(2)}_{att}(|\mathbf{r}' - \mathbf{r}|)$ is defined as

$$\Delta C^{(2)}_{att}(|\mathbf{r}' - \mathbf{r}|) = \Delta C^{(2)}_{Y}(|\mathbf{r}' - \mathbf{r}|) - \Delta C^{(2)}_{hs}(|\mathbf{r}' - \mathbf{r}|) \quad (15)$$

where $\Delta C^{(2)}_{hs}(|\mathbf{r}' - \mathbf{r}|)$ is the second-order DCF of a HCY fluid, which is given by the Percus−Yevick approximation of the Ornstein−Zernike (OZ) equation.

$$\Delta C^{(2)}_{hs}(r) = \begin{cases} 0 & r > \sigma \\ -a_{hs} - b_{hs}(r/\sigma) - \dfrac{\eta}{2} a_{hs}(r/\sigma)^3 & r < \sigma \end{cases} \quad (16)$$

The parameters a_{hs} and b_{hs} for hard-sphere fluid are

$$a_{hs} = \frac{(1 + 2\eta)^2}{(1 - \eta)^4} \quad (17)$$

$$b_{hs} = -6\eta \frac{(1 + \eta/2)^2}{(1 - \eta)^4} \quad (18)$$

$\Delta C^{(2)}_{Y}(|\mathbf{r}' - \mathbf{r}|)$ is the second-order DCF of a HCY fluid, which can be obtained, for example, from numerical solutions of HNC or first-order mean spherical approximation (MSA)[29] closure of the OZ equation. The most popular approach is to calculate $\Delta C^{(2)}_{Y}(|\mathbf{r}' - \mathbf{r}|)$ from the MSA,[30,31] due to its analytical expressions in reasonable accuracy:

$$\Delta C^{(2)}_{Y}(r) = -a - \frac{b}{\sigma} r - \frac{a r^3}{2\sigma^3} - \frac{\upsilon\sigma}{\lambda r}(1 - e^{-\lambda r/\sigma}) - \upsilon^2 \frac{\cosh(\lambda r/\sigma) - 1}{2\lambda^2 e^{\lambda} r/(\sigma T^*)} \quad (19)$$

for $r < 0$ and

$$C^{(2)}_{Y}(r) = \frac{\sigma}{T^* r} \exp[-\lambda(r - \sigma)/\sigma] \quad (20)$$

for $r > 0$. The parameters a, b, and υ in eq 19 are three functions of density ρ, reduced temperature $T^* = kT/\epsilon$, and screening parameter λ, and can be obtained by solving three coupled nonlinear equations.

The density profiles are solved from eq 14 using the Picard-type iterative method. The iteration starts with the corresponding bulk density as an initial guess. The next input is obtained by mixing the new density profile with the previous one. The numerical integrations are performed using the trapezoidal rule with the step size Δz or $\Delta r = 0.005\sigma$. The iteration repeats until the percentage change is smaller than 0.001 at all points.

III. Monte Carlo Simulations

Besides the simulation data from the literature, grand canonical ensemble Monte Carlo (GCMC) simulations are carried out in this work to test the performance of the DFT for attractive and repulsive HCY fluid at different temperatures and bulk densities. Before the GCMC, Widom test particle method in an *NVT* ensemble is used to determine the excess chemical potential as a function of the bulk density and temperature. The conventional Metropolis algorithm is used for generating successive configurations with the probability of successful displacement adjusted to 50%. At each density and temperature, the simulation box contains 1001 particles. In each MC cycle, all particles are displaced once, and then a test Yukawa molecule is inserted into the system five times to obtain excess chemical potential because this may enable phase space to be covered more efficiently if an appropriate value for the maximum displacement is chosen.[32]

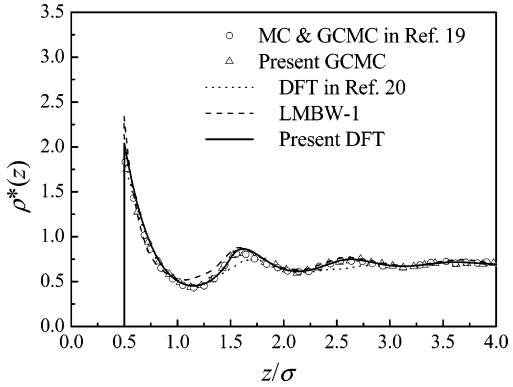

Figure 1. Comparison of density profiles from different methods for an attractive Yukawa fluid near a hard wall at reduced density $\rho^* = 0.7$ and reduced temperature $T^* = 2.0$. The open circles and triangles represent the Monte Carlo simulation results from Olivares-Rivas et al.[19] and the present work, respectively. The dotted, dashed, and solid lines refer to the results from the DFT of Yi and Kim,[20] LMBE-1 equation,[19] and present DFT, respectively.

The grand canonical Monte Carlo (GCMC) simulation is then carried out with the excess chemical potential obtained above. The simulation systems were constituted by two parallel walls separated by 10σ. The simulation box is cubic ($10\sigma \times 10\sigma \times 10\sigma$). The usual periodic boundary conditions and minimum imagine conventions were applied in the directions parallel to the walls. The cutoff distance of the Yukawa potential is set to 5σ. Beyond this distance, the Yukawa potential is smaller than $-1.4932 \times 10^{-4}/T^*$. At each density and temperature the simulation is run for 2.4×10^7 complete cycles for sampling the density distributions after about 1×10^6 cycles for equilibration. The density profile is recorded by dividing the region between the walls into a number of equal-sized bins. It is obtained by averaging the number of spheres in the bin over the length of the run.

IV. Results and Discussions

A. Attractive HCY Fluid near a Wall. We first discuss the density profiles of an attractive HCY fluid near a wall at different temperatures and densities. The external potential can be expressed as an exponential tail,

$$V_{ext}(z) = \begin{cases} \infty & z < \sigma/2 \\ -\epsilon_W \exp[-\lambda(z - \sigma/2)/\sigma] & z > \sigma/2 \end{cases} \quad (21)$$

where ϵ_W is the energy parameter of the wall. Throughout this work, the hard-sphere Yukawa potential with the range parameter $\lambda = 1.8$ is used. To test the performance of our GCMC simulations and the DFT equations, we compare in Figure 1 the density profiles from different methods for the attractive HCY fluid near a hard wall at reduced density $\rho^* = 0.7$ and reduced temperature $T^* = kT/\epsilon = 2.0$. As expected, our GCMC results are in excellent agreement with that of Olivares-Rivas et al.,[19] demonstrating that our GCMC program is correct and reliable. Also included in Figure 1 are results from the DFT of Yi and Kim,[20] from the LMBW-1 integral equation,[19] and from the present DFT. The DFT of Yi and Kim[20] gives correct contact value, while it underestimates the strength of the oscillation of the density profile. The density profile from the present DFT is better than those from the LMBW-1 integral equation and the DFT of Yi and Kim.[20] In addition, the present DFT has the

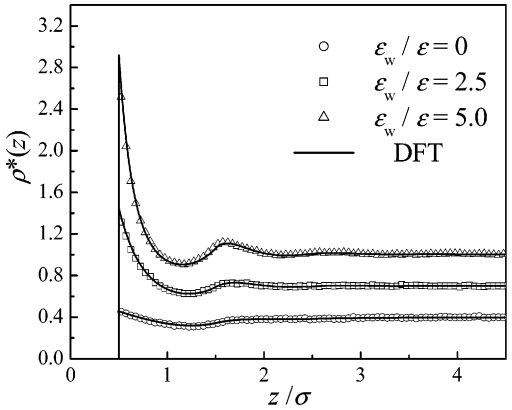

Figure 2. Reduced density profiles for an attractive Yukawa fluid near a wall at reduced density $\rho_b\sigma^3 = 0.4$ and reduced temperature $T^* = 2.0$. The symbols and solid curves represent the results from the GCMC simulation and present DFT, respectively. To enhance visual clarity, the profiles of $\epsilon_W/\epsilon = 2.5$ and 5.0 are shifted upward by 0.3 and 0.6, respectively.

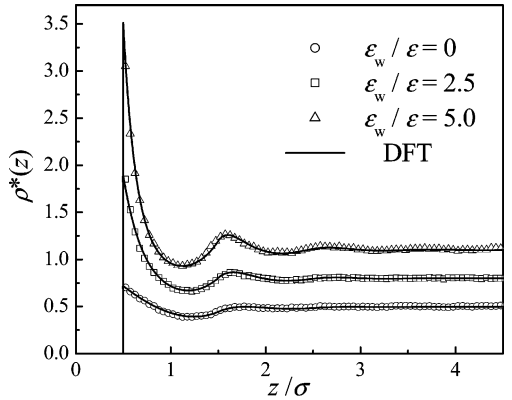

Figure 3. Same as in Figure 2 but for reduced density $\rho_b\sigma^3 = 0.5$.

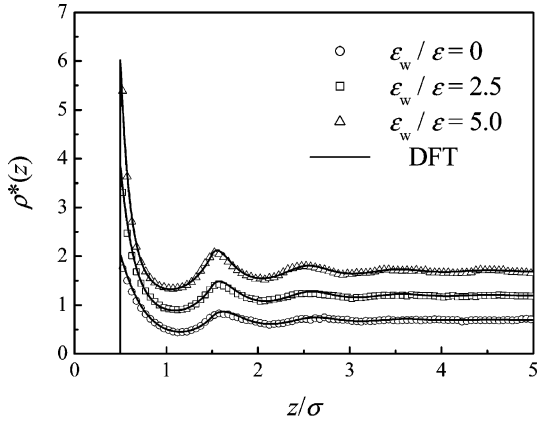

Figure 4. Reduced density profiles for an attractive Yukawa fluid near a wall at reduced density $\rho_b\sigma^3 = 0.7$ and reduced temperature $T^* = 2.0$. The symbols and solid curves represent the results from the GCMC simulation and the present DFT, respectively. To enhance visual clarity, the profiles of $\epsilon_W/\epsilon = 2.5$ and 5.0 are shifted upward by 0.5 and 1.0, respectively.

advantage of numerical simplicity because no parameter has to be chosen to satisfy the correct total pressure of the homogeneous fluid.

In Figures 2−4, the density profiles predicted from the present DFT are compared with those from the GCMC simulations carried out in this work for the attractive HCY fluid near a wall at temperature $T^* = 2.0$ and reduced densities $\rho\sigma^3 = 0.4$, 0.5, and 0.7, respectively, and for each density, three wall energy parameters $\epsilon_W/\epsilon = 0$, 2.5, and 5.0 are considered. At this

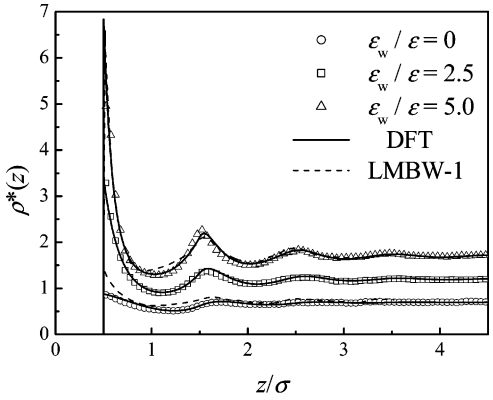

Figure 5. Same as in Figure 4 except that the dotted lines refer to the results from the LMBW-1 equation[19] and the reduced temperature is $T^* = 1.25$.

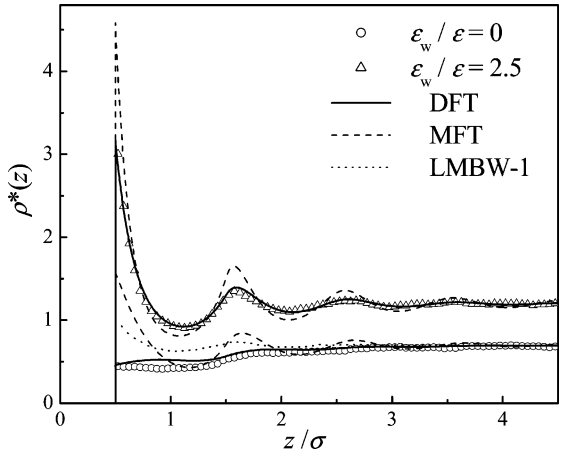

Figure 6. Reduced density profiles for an attractive Yukawa fluid near a wall at reduced density $\rho_b\sigma^3 = 0.7$ and reduced temperature $T^* = 1.1$. The symbols, dashed, dotted, and solid lines represent the results from the GCMC simulation, MFT, LMBW-1 equation,[19] and present DFT, respectively. To enhance visual clarity, the profiles of $\epsilon_W/\epsilon = 2.5$ are shifted upward by 0.5.

temperature, the present DFT provides density profiles that are in excellent agreement with the GCMC simulation results. It can be seen from Figures 2−4 that the higher the wall energy parameter ϵ_W is, the larger the magnitude of density oscillation. The density profiles shift toward the wall as density increases. There is a significant accumulation of spheres near the wall at high density and large value of ϵ_W.

For reduced density $\rho\sigma^3 = 0.7$ and reduced temperatures $T^* = 1.25$ and 1.1, the HCY fluid is near the vapor−liquid transition temperature. When $\epsilon_W = 0$, the density profiles have fewer oscillations and approach monotonic, as shown in Figures 5 and 6. The depletion of attractive HCY fluids near a wall at low temperature ($T^* = 1.1$) is the result of the competition between excluded-volume and attractive interaction: the former favors accumulation of spheres near the wall, while the latter restricts the sphere close to the wall. At low temperature, the attractive interaction prevails and the density profile shows depletion. The comparisons with the GCMC simulation data suggest that the density profiles predicted from the present DFT are in good agreement with the corresponding simulation data. In contrast, the LMBW-1 equation[19] overestimates the density at contact and gives incorrect oscillatory behaviors, as can be seen in Figure 6. The MFT used here for Yukawa fluid is implemented by using the MFMT[3,4] for the repulsive functional. Figure 6 shows that the MFT is not only quantitatively unreliable but also qualitatively questionable due to its failure to describe

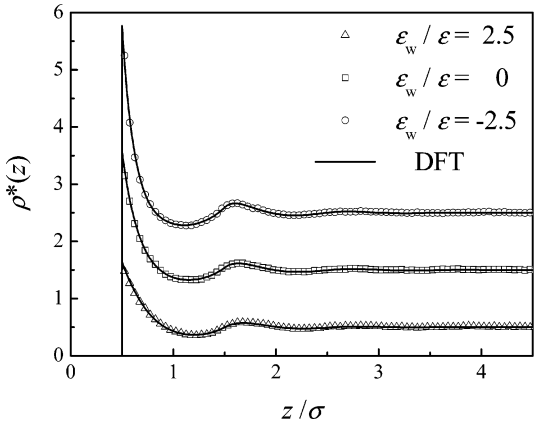

Figure 7. Reduced density profiles for a repulsive Yukawa fluid near a wall at reduced density $\rho_b\sigma^3 = 0.5$ and reduced temperature $T^* = -2.0$. The symbols and solid curves represent the results from the GCMC simulation and the present DFT, respectively. To enhance visual clarity, the profiles of $\epsilon_W/\epsilon = 0$ and 2.5 are shifted upward by 1.0 and 2.0, respectively.

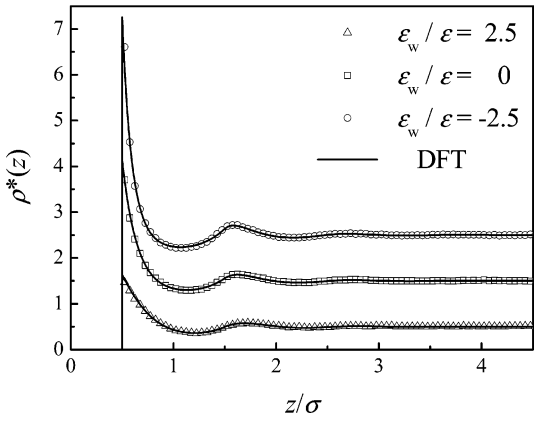

Figure 8. Reduced density profiles for a repulsive Yukawa fluid near a wall at reduced density $\rho_b\sigma^3 = 0.5$ and reduced temperature $T^* = -1.25$. The symbols and solid curves represent the results from the GCMC simulation and the present DFT, respectively. To enhance visual clarity, the profiles of $\epsilon_W/\epsilon = 0$ and 2.5 are shifted upward by 1.0 and 2.0, respectively.

the depletion near the wall at low temperature. In addition, the MFT gives too strong density oscillation. All these disadvantages are caused by its neglect of the structured free-energy functional, while the DCF is included to represent the structure in the present DFT.

B. Repulsive HCY Fluid near a Wall. Figures 7−9 present the density distributions of repulsive HCY fluids near a wall with a repulsive, attractive, or no forces at different densities ($\rho\sigma^3 = 0.5$ and 0.7) and temperatures ($T^* = -1.25$ and -2.0). The present DFT predicts accurate peak positions and contact density values. Figures 7−9 suggest that the present DFT gives more accurate density profiles for repulsive HCY fluid than that for the attractive case at all the conditions studied in this work. A remarkable difference is observed between the attractive and repulsive HCY fluids, indicating that the effect of confinement is enhanced for the repulsive HCY fluid. As we know, the density profiles of attractive HCY fluid oscillate with a periodicity of a hard-sphere diameter σ. However, a longer periodicity of density oscillation is observed for the repulsive HCY fluids, as can be seen from Figures 7−9. Furthermore, no depletion phenomena are found for the repulsive HCY fluid near the wall with attractive or repulsive forces, because both excluded-volume effect and repulsive interaction favor accumulation of spheres near the wall.

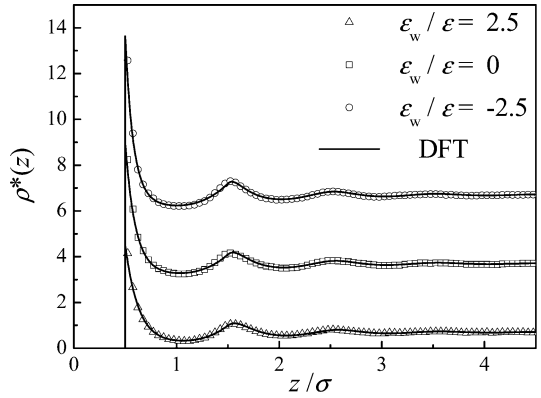

Figure 9. Reduced density profiles for a repulsive Yukawa fluid near a wall at reduced density $\rho_b\sigma^3 = 0.7$ and reduced temperature $T^* = -2.0$. The symbols and solid curves represent the results from the GCMC simulation and the present DFT, respectively. To enhance visual clarity, the profiles of $\epsilon_W/\epsilon = 0$ and 2.5 are shifted upward by 3.0 and 6.0, respectively.

In general, the quadratic density expression becomes unreliable when the local density is significant from the bulk density. However, in Figures 2−5 the present DFT only slightly overestimates the contact value of density at the strongly attractive surface ($\epsilon_W/\epsilon = 5$). The possible reason for the good results is that the errors from all the neglected higher-order terms are canceled out by the approximation of the used direct correlation function. Since the vapor−liquid interface is less inhomogeneous than the systems studied here, the quadratic density expansion should be more accurate, and we hope that the present DFT may predict the vapor−liquid interfacial properties equally well.

C. Radial Distribution Function of HCY Fluid. On the basis of the idea of Percus' test-particle method, the present DFT can be used to calculate the radial distribution functions of the bulk HCY fluid. If we fix a sphere, then the external potential produced by the fixed sphere is given by

$$V_{ext}(r) = \begin{cases} \infty & r < \sigma \\ -\dfrac{\epsilon\sigma \exp[-\lambda(r/\sigma - 1)]}{r} & r \geq \sigma \end{cases} \tag{22}$$

If the density profile of other spheres around the fixed particle is calculated from the DFT, the radial distribution function $g(r)$ can be obtained through

$$g(r) = \rho(r)/\rho_b \tag{23}$$

Equation 23 has been applied to attractive and repulsive HCY fluids. Figure 10 depicts the predicted radial distribution functions for the attractive HCY fluid at reduced temperature $T^* = 2.0$ and reduced densities $\rho\sigma^3 = 0.3$ and 0.8, along with the Monte Carlo data of Shukla.[12] The agreement between the present DFT and the computer simulation is excellent. The contact values of the radial distribution functions from the present DFT are very accurate for attractive HCY fluids. The excellent agreement can also be achieved from Figure 11 at a subcritical temperature $T^* = 1.0$ and a reduced density $\rho\sigma^3 = 0.8$. When Figures 10 and 11 are compared with the Figures 4 and 5 in ref 25, we found that the present DFT gives a more accurate radial distribution function than Zhou's perturbation DFT[25] does. Furthermore, our DFT is simpler in calculation than that of Zhou because we avoid the determination of the parameter from the bulk pressure.

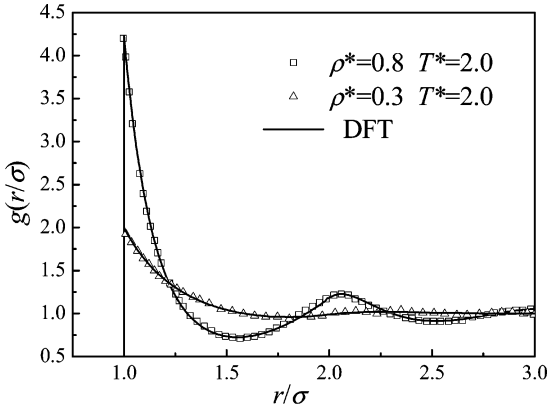

Figure 10. Radial distribution functions of an attractive Yukawa fluid at reduced temperature $T^* = 2.0$. The symbols and solid lines represent the results from simulation[12] and the present DFT, respectively.

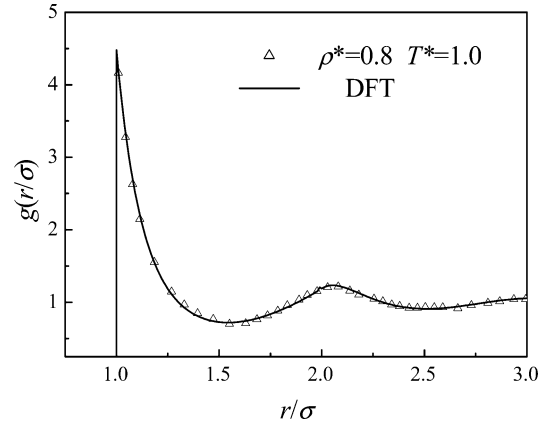

Figure 11. Radial distribution functions of an attractive Yukawa fluid at reduced temperature $T^* = 1.0$ and reduced density $\rho^* = 0.8$. The symbols and solid line represent the results from simulation[12] and the present DFT, respectively.

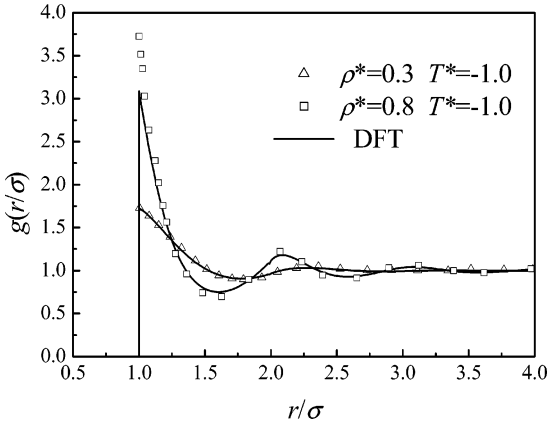

Figure 12. Radial distribution functions of a repulsive Yukawa fluid at reduced temperature $T^* = -1.0$. The symbols and solid line represent the results from the simulation[18] and the present DFT, respectively.

To check the applicability of the present DFT to the structure of bulk repulsive HCY fluid, we compare in Figure 12 the predicted radial distribution function with the Monte Carlo simulation data of Cochran and Chiew[18] at reduced temperature $T^* = -1.0$ and reduced densities $\rho\sigma^3 = 0.5$ and 0.8. While the agreement between the present DFT and the simulation is excellent at low density ($\rho\sigma^3 = 0.5$), the accuracy of the theory becomes poor especially in the vicinity of contact. The present DFT substantially underestimates the contact value of the radial distribution function for the repulsive HCY fluid at high density. The poor performance of the present DFT at high density is probably due to the inaccuracy of the MSA solution for the direct correlation function of the repulsive HCY fluid at high density. A possible improvement of the present DFT is to use the more accurate DCF obtained from the self-consistent integral equation.[33,34]

V. Conclusions

We have applied the grand canonical ensemble Monte Carlo simulation and a proposed density functional theory (DFT) to investigate the structures of attractive and repulsive hard-core Yukawa fluids near a wall as well as the radial distribution function of the bulk hard-core Yukawa fluids. The perturbative method proposed by Rosenfeld[26] is used to treat the attractive functional by making use of the direct correlation function of the corresponding bulk fluid. The hard-sphere contribution to the free-energy functional of hard-core Yukawa fluid is evaluated from the modified fundamental measure theory of Yu and Wu,[3,4] and the attractive contribution is approximated by a quadratic expansion with respect to the corresponding bulk fluid. The direct correlation function used in the attractive functional is the analytical solution of the mean spherical approximation for the hard-core Yukawa fluid. The method proposed here is simple in form and easy to implement.

Extensive comparison with GCMC simulation results for the density profiles of attractive and repulsive hard-core Yukawa fluids near a wall indicates that the current theory is fairly accurate. The present DFT is capable of describing the surface depletion of attractive hard-core Yukawa fluids. It has a significant improvement on those of the modified version of the Lovett−Mou−Buff−Wertheim (LMBW-1)[19] and the perturbative method of Yi and Kim.[20] In contrast, the widely used mean field theory gives too strong density oscillation and fails to account for the depletion. Therefore, the DFT proposed in this work is comprehensively reliable and computationally efficient. Furthermore, from both the simulation and present DFT we know that the repulsive hard-core Yukawa fluid, which presents a purely repulsive interaction between like-charged colloidal particles, has no depletion near a wall.

When the present DFT is applied to the calculation of the radial distribution function, good results are obtained for the attractive hard-core Yukawa fluids. For the repulsive case, the present DFT predicts very accurate radial distribution functions at low density, but overestimates the radial distribution functions in the vicinity of contact at high density. This shortcoming can be overcome by using a more accurate direct correlation function in the attractive Helmholtz functional. It is concluded that the method used in this work is promising for practical applications such as colloidal suspensions in confined geometry, inhomogeneous dense plasmas, etc.

Acknowledgment. This work is sponsored by the National Natural Science Foundation of China (Grant No. 20376037 and 20490200). We are grateful to Dr. J. Z. Wu and Dr. Y.-P. Tang for useful discussion.

References and Notes

(1) Henderson, D. *Fundamentals of Inhomogeneous Fluids*; Dekker: New York, 1992.
(2) Rosenfeld, Y. *Phys. Rev. Lett.* **1989**, *63*, 980.
(3) Yu, Y.-X.; Wu, J. Z. *J. Chem. Phys.* **2002**, *117*, 10156.
(4) Yu, Y.-X.; Wu, J. Z.; Xin, Y.-X.; Gao, G.-H. *J. Chem. Phys.* **2004**, *121*, 1535.
(5) Roth, R.; Dietrich, S. *Phys. Rev. E* **2000**, *62*, 6926.
(6) Tang, Y. P.; Wu, J. Z. *Phys. Rev. E* **2004**, *70*, 011201.
(7) Shao, X. H.; Huang, S. P.; Wang, W. C. *Acta Chim. Sin.* **2003**, *61*, 1740.

(8) Gonzalez-Mozuelos, P.; Alejandre, J.; Medina-Noyola, M. *J. Chem. Phys.* **1991**, *95*, 8337.
(9) Fu, D.; Li, Z. C.; Li, Y. G.; Lu, J. F. *Acta Chim. Sin.* **2003**, *61*, 1561.
(10) Fu, D.; Lu, J.-F.; Wu, W.; Li, Y.-G. *Chin. J. Chem.* **2004**, *22*, 627.
(11) Bonaskarne, M.; Amokrane, S.; Regnant, C. *J. Chem. Phys.* **1999**, *111*, 2151.
(12) Shukla, K. P. *J. Chem. Phys.* **2000**, *112*, 10358.
(13) van Horn, H. M. *Science* **1991**, *252*, 384.
(14) Hasegawa, M. *J. Chem. Phys.* **1998**, *108*, 208.
(15) Gonzalez-Melchor, M.; Trokhymchuk, A.; Alejandre, J. *J. Chem. Phys.* **2001**, *115*, 3862.
(16) Duh, D.-M.; Mier-Y−Teran, L. *Mol. Phys.* **1997**, *90*, 373.
(17) Henderson, D.; Blum, L.; Nowortya, J. P. *J. Chem. Phys.* **1995**, *102*, 4973.
(18) Cochran, T. W.; Chiew, Y. C. *J. Chem. Phys.* **2004**, *121*, 1480.
(19) Olivares-Rivas, W.; Degreve, L.; Henderson, D.; Quintana, J. *J. Chem. Phys.* **1997**, *106*, 8160.
(20) Yi, J.-H.; Kim, S.-C. *J. Chem. Phys.* **1997**, *107*, 8147.
(21) Tarazona, P. *Phys. Rev. A* **1985**, *31*, 2672.
(22) Tarazona, P.; Bettolo Marconi, U. M.; Evans, R. *Mol. Phys.* **1987**, *60*, 573.
(23) Rickayzen, G.; Augousti, A. *Mol. Phys.* **1984**, *52*, 1355.
(24) Rickayzen, G.; Kalpaxis, P.; Chacon, E. *J. Chem. Phys.* **1994**, *101*, 7963.
(25) Zhou, S. *J. Phys. Chem. B* **2002**, *106*, 7674.
(26) Rosenfeld, Y. *J. Chem. Phys.* **1993**, *98*, 8126.
(27) Boublik, T. *J. Chem. Phys.* **1970**, *53*, 471.
(28) Mansoori, G. A.; Carnahan, N. F.; Starling, K. E.; Leland, T. W. J. *J. Chem. Phys.* **1971**, *54*, 1523.
(29) Tang, Y. P. *J. Chem. Phys.* **2004**, *121*, 10605.
(30) Henderson, D.; Stell, G.; Waisman, E. *J. Chem. Phys.* **1975**, *62*, 4247.
(31) Stell, G.; Sun, S. F. *J. Chem. Phys.* **1975**, *63*, 5333.
(32) Leach, A. R. *Molecular Modeling: Principles and Applications*; Addison-Wesley Longman Ltd.: London, 1996.
(33) Zerah, G.; Hansen, J.-P. *J. Chem. Phys.* **1986**, *84*, 2336.
(34) Rogers, F. J.; Young, D. A. *Phys. Rev. A* **1984**, *30*, 999.